Development of a hot tear indicator for steel castings

Charles Monroe, Christoph Beckermann *

Department of Mechanical and Industrial Engineering, University of Iowa, Iowa City, IA 5224, USA

Received in revised form 14 July 2005

Abstract

A hot tear indicator based on the physics of solidification and deformation is presented. This indicator is derived using available data from computer simulation of solidification and solid deformation. Hot tears form when the mushy zone is starved of liquid feeding and deformed in tension. The unfed tensile deformation causes a small additional porosity. A physical model based on a mass balance is developed to find the additional porosity formed. This additional porosity or porosity due to solid deformation (PSD) is a locator for initiation sites for hot tears in the casting, not a full tear predictor. Simulation results for various "T"-shaped steel castings show good agreement with previous experimental findings. Reducing the strain in the casting and increasing the feeding of the section are found to decrease the hot tear tendency.
© 2005 Elsevier B.V. All rights reserved.

Keywords: Hot tears; Casting simulation; Steel

1. Introduction

Once hot tears occur in steel castings, they must be repaired by welding or the casting must be scrapped. Considerable effort is spent to eliminate hot tears from castings. Hot tears are identified as cracks, either on the surface or internally in the casting. These cracks may be large and visible to the naked eye or small and found only by magnetic particle inspection. They are caused by a combination of thermal effects, such as hot spot size and casting restraint, such as cores in cylindrical castings [1]. In addition, composition can affect hot tearing tendency [2]. Physically, two factors contribute to hot tearing in the mushy zone. Hot tears are formed when the mushy zone is cut off from liquid feeding and is under tensile loading [3].

Liquid feeding flows are induced by the contraction of liquid steel during cooling and shrinkage upon solidification. The friction that the liquid experiences, as it flows through the mush creates a significant pressure drop, such that the pressure deep inside the mushy zone is close to vacuum. Such a vacuum can also form inside a hot spot region, even if the solid fraction is still small. If the pressure is sufficiently small, porosity can form. In steel, the amount of dissolved gases is typically very small. Therefore, any porosity formation will signal that the feeding flow is cut off.

Mechanical loading, tensile or compressive, is caused by restrained thermal contraction. Restraint is the consequence of cores, geometry constraints and other factors, which act to resist the movement of the casting surface during solidification. To accommodate the restraint of a surface, mechanical strains are generated inside the casting. It is these mechanical strains and not the thermal strain that can transmit the compressive or tensile loads. In the mushy zone, the individual solid and liquid phases are incompressible but the mixture is compressible, as noted by Martin et al. [4]. In compression, liquid is squeezed out. In tension, liquid may be sucked in. If liquid is not available under tensile loading, due to the feeding flow being cut off, additional porosity may form. This porosity forms late in solidification, along grain boundaries. It is the initiation site for a hot tear and is referred to in this study as porosity due to solid deformation (PSD).

Experimental work by the Steel Founders' Society of America (SFSA) [5] demonstrated the effect of casting design on hot tearing. By changing various section lengths and thicknesses of a "T"-shaped steel casting, the effects of variation in hot spot size and strain on hot tearing was investigated. It was concluded that hot tears could be avoided by using filleted corners, smaller section size transitions and an unrestrained casting and gating layout. These methods enhance liquid feeding and reduce the tensile strain in the casting.

Numerous hot tear indicators have been reported in the literature. Critical strain has been one measure of hot tearing susceptibility [6]. However, the critical strain is dependent on

---

* Corresponding author. Tel.: +1 319 335 5681; fax: +1 319 335 5669.
E-mail address: becker@engineering.uiowa.edu (C. Beckermann).

many other parameters, such as the availability of liquid metal feeding and strain rate and cannot be used alone as an indicator of hot tears [7]. A recently developed, physically based indicator is the RDG criterion developed by Rappaz et al. [3]. The RDG criterion is derived using a mass balance on a solidifying mushy zone. The mass balance is solved for the maximum sustainable strain rate. This is the strain rate beyond which cavitation or porosity formation occurs. The authors show that this criterion agrees with the well-known "Λ curves" for hot tearing from phenomenological models and experimental results. These "Λ curves" are graphs of certain hot tear criteria against solute concentration. A peak is observed at a composition close to the maximum freezing range of an alloy. The model is developed using a one-dimensional domain, across the mushy zone and is thus, not immediately applicable to three-dimensional situations. The RDG criterion also is sensitive to the definition of the coherency temperature, i.e., the temperature at which the dendritic network can transmit stresses. In continuous casting, this criterion is useful because the strain rate is directly related to the casting speed. However, it is not clear how the RDG criterion can be applied to shaped castings.

Mo et al. [8] recently developed a two-phase model for hot tearing, where the energy, liquid and solid momentum and continuity equations are solved simultaneously. Similar to the RDG criterion, a hot tear criterion based on the liquid pressure drop is used. However, this model also has limitations because porosity formation is not considered. The authors demonstrate the sensitivity of the liquid pressure drop to strain rate, solid to liquid velocity coupling, solid constitutive equations, etc.

In the following section, the present hot tear indicator for shaped steel castings is developed and the method used for calculating the indicator as part of a casting simulation is described. Then, the "T"-shaped castings from the SFSA experiments [5] are simulated. The simulation results are compared to the measurements. Also, the effect of feeding a hot spot on hot tearing is demonstrated.

2. Method

The present hot tear indicator is calculated from the results of relatively standard casting simulations in a two-step process. As a first step, the equations for energy, liquid momentum, continuity and gas species are solved using the commercial software package MAGMAsoft [9]. Second, the MAGMAstress module, which uses temperature results from the first simulation, is employed to model the deformation. The results from both of these simulations are then used to form the present hot tear indicator. The advantage of this methodology is that it is straightforward for industry to implement using available simulation technology. The disadvantage is that it is only an approximate solution to this coupled problem.

The solution in the first step is based on the multi-phase model for porosity formation developed by Carlson et al. [10] and implemented within MAGMAsoft. This model calculates the porosity formation and final distribution in the casting due to volume changes, but considers feeding by the liquid phase only. The solid is assumed to be rigid and stationary.

The stress analysis in the second step is based on a standard small-strain, thermo-elastic formulation that considers both the metal and the mold. This simulation yields the stresses and the thermal and elastic strains and strain rates in the solidifying casting geometry. The neglect of inelastic contributions to the total strain is believed to be a reasonable approximation in the present application, because the stresses encountered are small. In steel casting, the extent of the mushy zone is relatively short and the thermal strains of the fully solid material (e.g., the shell) control the deformations during solidification. Since the fully solidified portions of a casting are much more rigid than the liquid or the mushy zone, the weaker areas will simply conform to the thermal contractions of the adjacent solid. The mechanical properties of the mush are discussed later in this section.

The above two-step method decouples the liquid and solid phase movements inside the mushy zone. In the first step, any effect that solid deformation may have on the flow of the liquid in the mush and on the formation of porosity is neglected. In the second step, liquid flows and porosity formation are not considered when calculating the solid deformation. The coupling of all of these effects can be better understood by examining the complete statement of continuity or mass balance for the mushy zone. The mush is considered to be a mixture of three phases: solid metal (s), liquid metal (l) and porosity (p), such that the volume fractions add up to unity, i.e., $f_s + f_l + f_p = 1$. The volume averaged mixture continuity equation is then given by:

$$\frac{\partial}{\partial t}(f_s \rho_s + f_l \rho_l + f_p \rho_p) + \nabla \cdot (f_s \rho_s \boldsymbol{v}_s + f_l \rho_l \boldsymbol{v}_l + f_p \rho_p \boldsymbol{v}_p) = 0 \tag{1}$$

where t, ρ and $\boldsymbol{v}$ are time, density and velocity, respectively. Note that the densities of the three phases are all different. Hence, Eq. (1) states that changes in the volume fractions of any of the three phases inside a control volume can be balanced by mass fluxes of any of the three phases in or out of the control volume. If the phase volume fractions do not change, solid deformation ($\boldsymbol{v}_s \neq 0$) can be accommodated by flow of liquid. This full coupling of all effects cannot be accounted for with the present two-step solution procedure.

In order to make progress, the above mixture continuity equation is split into two parts: one that is solved as part of the porosity model of the first step and another one that only accounts for porosity formation due to solid deformation. This split is accomplished by defining the total pore fraction to consist of two components:

$$f_p = f_p^l + f_p^s \tag{2}$$

The first component, f_p^l, is referred to as porosity or original porosity and includes all contributions due to shrinkage and flow of liquid. The second component, f_p^s, is referred to as additional porosity or porosity due to the solid deformation and includes only contributions due to movement of solid. PSD is, thus, the porosity that is created or destroyed by solid deformation. It is this additional porosity that constitutes potential initiation sites for hot tears.

Substituting Eq. (2) into Eq. (1) and neglecting the terms associated with the pore density (i.e., $f_p \rho_p \boldsymbol{v}_p = 0$ and $f_p \rho_p = 0$), Eq. (1) is rearranged as follows:

$$\frac{\partial}{\partial t}(f_s(\rho_s - \rho_l) + \rho_l - f_p^l \rho_l) + \nabla \cdot (f_l \rho_l \boldsymbol{v}_l)$$

$$= \frac{\partial}{\partial t}(f_p^s \rho_l) - \nabla \cdot (f_s \rho_s \boldsymbol{v}_s) \tag{3}$$

A decoupling is now introduced by setting both sides of Eq. (3) equal to 0. The left side of Eq. (3), equal to 0, is the mixture continuity equation if the solid phase is assumed to be rigid and stationary; this continuity equation is solved for f_p^l as part of the multi-phase model for porosity formation in step one of the present solution procedure. Setting the left side equal to 0 requires a balance between the additional porosity f_p^s and the solid mass flux on the right side of Eq. (3). The consequence of this decoupling is that the solid deformation in the mushy zone has no effect other than to create or destroy additional porosity, i.e., solid deformation cannot squeeze out or pull in liquid. This decoupling is believed to be a good approximation for steel castings because hot tears form only when the liquid feeding flow is already cut off.

Setting the left side of Eq. (3) equal to 0 and assuming, as a first approximation that the liquid and solid metal densities are constant, yields:

$$\frac{\partial}{\partial t}(f_p^s) = \frac{\rho_s}{\rho_l} \nabla \cdot (f_s \boldsymbol{v}_s) \tag{4}$$

Eq. (4) must be integrated to find the porosity due to solid deformation. The integration is started at the point in time when the porosity increases from 0, i.e., $f_p^l > 0$. This time indicates when the liquid feeding is cut off and the pressure is low enough to form a pore. When liquid feeding is still available, solid deformation is not expected to create any porosity. The integration is stopped at the point in time when the mush is locally solidified, i.e., $T < T_s$. Further crack growth and propagation in the fully solidified material are not modeled by this approach. Using these integration limits, Eq. (4) becomes:

$$\mathrm{PSD} = f_p^s = \frac{\rho_s}{\rho_l} \int_{f_p^l > 0}^{T < T_s} \nabla \cdot (f_s \boldsymbol{v}_s) \mathrm{d}t \tag{5}$$

Eq. (5) states that the local solid dilatation, after liquid feeding is cut off, will cause PSD formation. The local solid dilatation rate is found from the stress analysis in the second step of the present solution procedure. As noted in Section 1, the thermal contractions of the mushy zone do not contribute to the deformation of the solid, but only to liquid feeding. Therefore, only the mechanical strains and strain rates are used in the calculation of PSD. The solid velocity multiplied by the solid fraction is known as the superficial velocity. As a first approximation, the divergence of this superficial velocity is identified with the trace of the mechanical strain rate tensor, i.e.,

$$\nabla \cdot (f_s \boldsymbol{v}_s) = \mathrm{trace}(\dot{\varepsilon}^{\mathrm{m}}) = \dot{\varepsilon}_{xx}^{\mathrm{m}} + \dot{\varepsilon}_{yy}^{\mathrm{m}} + \dot{\varepsilon}_{zz}^{\mathrm{m}} \tag{6}$$

The superscript m denotes that only the mechanical contribution of the strain is used. Substituting Eq. (6) into Eq. (5), the final

expression for PSD is given by:

$$\mathrm{PSD} = f_p^s = \frac{\rho_s}{\rho_l} \int_{f_p^l > 0}^{T < T_s} [\dot{\varepsilon}_{xx}^{\mathrm{m}} + \dot{\varepsilon}_{yy}^{\mathrm{m}} + \dot{\varepsilon}_{zz}^{\mathrm{m}}] \mathrm{d}t \tag{7}$$

Eq. (7) constitutes the present hot tear indicator. The integration of the strain rates over time in Eq. (7) shows that PSD is nothing but a volumetric strain. However, PSD is more than an indicator that is solely based on the notion of a critical strain for hot tear formation [6,7]. Because the integration is started at the point in time when the regular porosity starts to form ($f_p^l > 0$), PSD accounts for the effect of liquid feeding. This is critical for the prediction of hot tears in shaped castings. Since liquid feeding is affected by many factors, including the freezing range and the permeability of the mush [10], PSD should yield predictions that are not dissimilar to the ones from the RDG criterion developed by Rappaz et al. [3]. Note that Eq. (7) does not explicitly contain the coherency temperature, consideration of grain boundaries or other effects associated with the structure of the mush; these parameters must generally be accounted for in the mechanical model (i.e., the constitutive equation) for the mush that is used to calculate the strain rates in Eq. (7).

It must be emphasized that the PSD found through Eq. (7) provides only an indication for the initiation of hot tears in the mushy zone. It does not predict tear or crack growth and the extent of a hot tear in the solidified casting at room temperature. The appearance of a crack can change the course of stress development in the casting during cooling. For example, if a hot tear develops at a certain location in a casting, stresses may be relieved and hot tears may not appear in other areas of the casting. However, the PSD indicator given by Eq. (7) can provide the initiation sites for hot tears and the locations with the greatest relative PSD percentages can be expected to have the greatest potential for hot tears.

The standard MAGMAstress module is used in the present study to calculate the mechanical strain rates for use in Eq. (7). This module requires the specification of the thermal expansion coefficient and the mechanical properties as a function of temperature throughout the casting process. Here, only the properties for the mush are discussed. The thermal expansion coefficient is found using the mixture density, $\bar{\rho} = f_s \rho_s + (1 - f_s)\rho_l$, where the individual phase densities and the solid fraction are given as a function of temperature. The relationship between the density and the thermal expansion coefficient is:

$$\alpha = -\frac{1}{\bar{\rho}} \frac{\partial \bar{\rho}}{\partial T} \tag{8}$$

Full consideration of the complex mechanical behavior of the mush as a function of its structure and coherency [4] is beyond the scope of the present study. As discussed in Section 1, the mush must generally be viewed as a compressible mixture. A standard viscoplastic constitutive model for an incompressible material could not be used to describe the mechanical behavior of the mush, because it would yield a zero trace of the strain rate tensor and, hence, no PSD. In the MAGMAstress module utilized here, the same elastic model is used for the mush as for the fully solid regions. The elastic modulus for the mush is

assumed to obey a law of mixtures such that $E = f_s E_s$, where E_s is the elastic modulus at the temperature T_s (100% solid). In other words, the mush is assumed to behave like a sponge where the solid provides the stiffness and the liquid is allowed to flow in or out. As the solid fraction approaches 0 and in the fully liquid, a small minimum value for E is used to avoid singularities in the stress calculations. A non-zero trace of the strain rate tensor is obtained in an elastic analysis for a Poisson ratio that is different from 1/2. This property of an elastic material is used here to model the compressibility of the mush. The Poisson ratio is simply assumed to be the same as for the fully solid. Due to this very approximate treatment of the mechanical behavior of the mush, the calculated trace of the strain rate tensor in the mush is likely to be inaccurate. However, hot tearing susceptibility can still be evaluated by comparing the relative magnitude of the PSD values, as shown below.

3. Simulation setup

The present hot tear indicator is validated using the "T"-shaped steel casting experiments of Ref. [5]. The composition of the steel was 0.23% carbon, 0.5% silicon, 0.6% manganese, 0.028% sulfur and 0.016% phosphorus. Fig. 1 shows a schematic of the casting geometry. The two ends of the arm were mechanically fixed in the mold, resulting in a zero displacement condition at the ends. Due to the contractions during cooling of the cast-

ing, this creates a large amount of thermal strain in the arm. The strain is concentrated in the center of the arm (i.e., at the mid-length) by the addition of the leg. The leg creates an unfed hot spot in the center of the "T", such that any hot tears would be expected at that location. In all cases, the thickness of the "T" was 1.0″ (2.54 cm).

Nine "T"-shaped castings were simulated with the following changes in the geometry. The arm length was either 26″ (66.04 cm) or 36″ (91.44 cm); lengthening the arm increases the amount of strain in the hot spot region. The arm width, dimension 'C' in Fig. 1, was increased from 0.5″ (1.27 cm) to 1.0″ (2.54 cm) and then to 2.0″ (5.08 cm); this increases the strength of the arm by providing more material to tear. The leg width, dimension 'E' in Fig. 1, was increased from 1.0″ (2.54 cm) to 2.0″ (5.08 cm); this increases the hot spot size at the section transition. These geometry changes constitute a total of eight test cases, as summarized in Table 1. An additional test case was created by placing a riser on top of the leg section of test casting 8 (see Table 1); this ninth case illustrates the effect of feeding on hot tearing.

Fig. 2 shows the casting simulation geometry for the three cases with a 36″ (91.44 cm) arm length (cases 7–9). The castings were gated at the end of the leg section using a runner that was 0.5″ (1.27 cm) thick and 1″ (2.54 cm) wide. At the end of the runner, a small riser, 2″ (5.08 cm) in diameter, was used to affect the filling of the mold and create a connection to the atmosphere
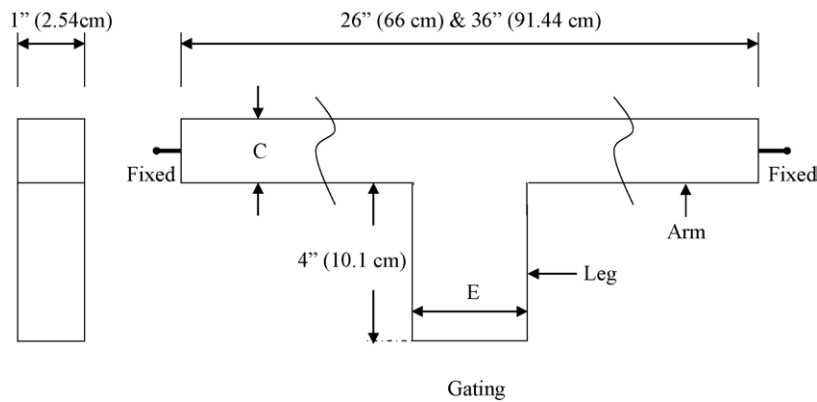

Fig. 1. Schematic of "T"-shaped casting [5].

Table 1
Summary of hot tearing predictions and experimental results for the "T"-shaped steel castings of Ref. [5]

| No.	Arm length	Arm width, 'C'	Leg width, 'E'	PSD average (%)	Casting result [5]
1	26″ (66)	0.5″ (1.27)	1.0″ (2.54)	**2.247**	**Heavy tear**
2	26″ (66)	0.5″ (1.27)	2.0″ (5.08)	**1.724**	**Tears**
3	26″ (66)	1.0″ (2.54)	1.0″ (2.54)	0.742	Untorn
4	26″ (66)	1.0″ (2.54)	2.0″ (5.08)	1.334	Untorn
5	26″ (66)	2.0″ (5.08)	1.0″ (2.54)	0.762	Untorn
6	26″ (66)	2.0″ (5.08)	2.0″ (5.08)	1.087	Untorn
7	36″ (91.4)	1.0″ (2.54)	1.0″ (2.54)	0.923	Untorn
8	36″ (91.4)	1.0″ (2.54)	2.0″ (2.54)	**1.530**	**Heavy tear**
9	36″ (91.4)	1.0″ (2.54)	2.0″ (2.54) w/riser	0.780	
Using coherency temperature integration limit					
8b	36″ (91.4)	1.0″ (2.54)	2.0″ (2.54)	1.589	
9b	36″ (91.4)	1.0″ (2.54)	2.0″ (2.54) w/riser	1.564	

Values in parentheses are in cm.
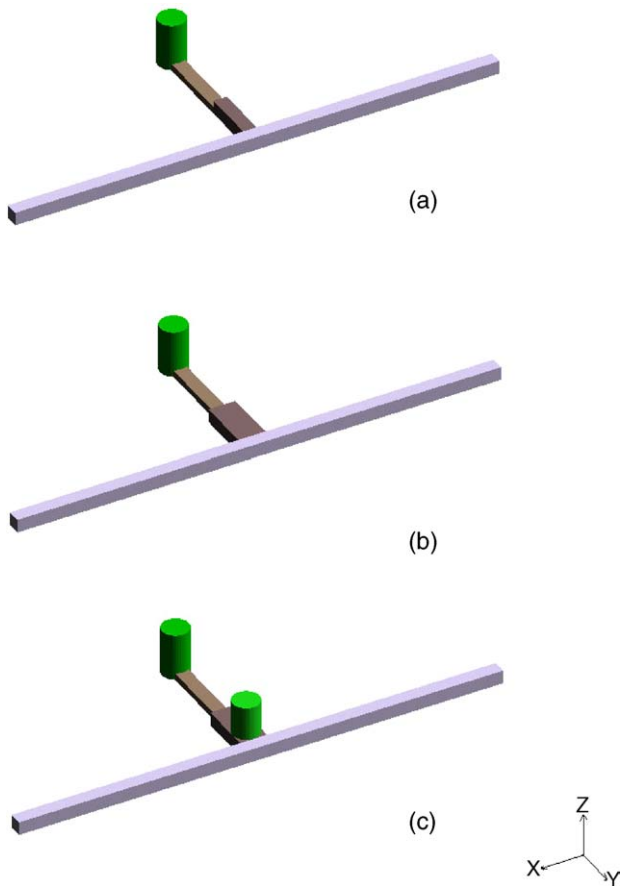
Fig. 2. Casting and gating geometry for a 36″ (91.44 cm) arm length and leg widths of: (a) 1.0″ (2.54 cm); (b) 2.0″ (5.08 cm); (c) 2.0″ (5.08) with riser.

surrounding the sand mold. The runner freezes off within a short time after filling, such that the riser at the end of the runner plays no role in the feeding of the "T" section. The riser on top of the leg in case 9 (Fig. 2c) is, however, intended to feed the hot spot at the center of the "T" section.

4. Results and discussion

An example of a predicted porosity distribution from the first step of the present simulation methodology is shown in Fig. 3a. This porosity, denoted as f_p^l in Section 2, is solely due to solidification shrinkage and the lack of feeding. As expected, a large amount of porosity, up to about 30%, can be observed in the leg section at the location of the hot spot. In addition, strong centerline porosity is present throughout the arm. Recall that the local time when this porosity starts to form during solidification constitutes the lower integration limit for calculation of the present hot tear indicator, PSD, as given by Eq. (7). An example of the predicted deformation from the second step of the present method is shown in Fig. 3b. This result corresponds to the point in time when the casting is just solidified. The deformation is magnified by 20 times to highlight the deflections. The predicted distortion pattern shows that the area of the bar near the hot spot is in tension due to the convex bending. In the following, the calculated PSD results are presented for each of the cases in
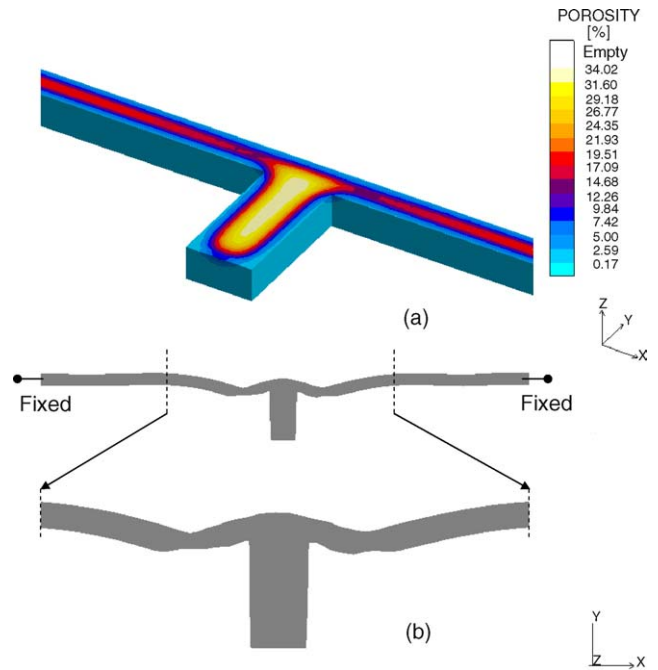

Fig. 3. Predicted MAGMAsoft results for a 36″ (91.44 cm) bar length and leg width of 2.0″ (5.08 cm) at fully solid: (a) distribution of porosity, f_p^l, neglecting solid deformation and (b) deformation magnified by a factor of 20.

Table 1 and compared to the corresponding casting experiments from Ref. [5].

4.1. Effect of geometry changes

Example casting trial results are provided in Fig. 4 for cases 7 and 8. The photograph shows that a heavy hot tear developed in the hot spot of the casting with the larger leg width (case 8, top), while the casting with the smaller leg width (case 7, bottom) is untorn. The formation of the hot tear can be explained by the fact that the large leg in case 8 keeps the center section partially liquid for a longer time than in case 7. During this time, the arm experiences a large strain at the location of the hot spot, which leads to the hot tear.

The corresponding simulation results for cases 7 and 8 are shown in Fig. 5. This figure is an X-ray view showing only indications of PSD that are 0.5% and greater, cut at mid-plane. The scale in figure is 0–6% PSD. It can be seen that for case
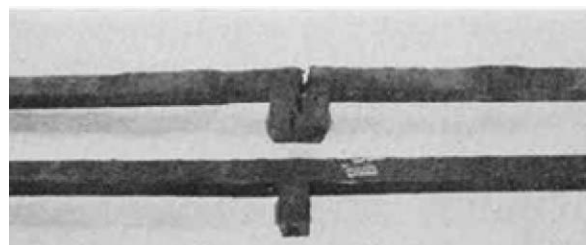

Fig. 4. Example casting trial results for a 36″ (91.44 cm) arm length and 1.0″ (2.54 cm) arm width; the casting at the top with a leg width of 2.0″ (5.08 cm) shows a heavy tear, while the casting at the bottom with a leg width of 1.0″ (2.54 cm) is untorn [5].
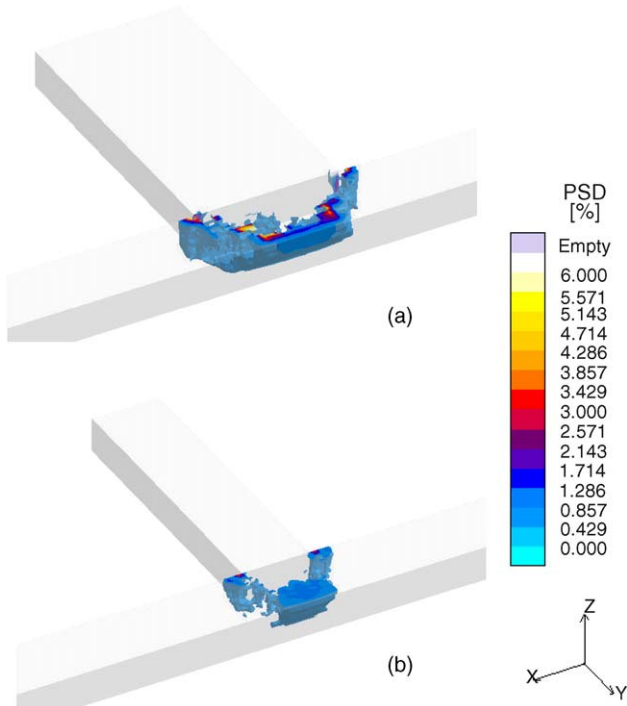
that the PSD indications will not look like the final hot tear from the experiment. This is because PSD is only an initiation site locator for hot tears and not a crack prediction.

In order to characterize and rank the PSD predictions for each simulation, an average PSD value is calculated by integrating all PSD values above 0.5% over the entire casting. Thus, only the PSD values visible in the X-ray views of Fig. 5 (and similar figures for the other cases) are used in forming the average. Table 1 provides the average PSD values for all cases. It can be seen that PSD averages above approximately 1.5% correspond to castings with hot tears, while for PSD averages below that value, no hot tears were observed in the casting experiments. It is emphasized that the actual magnitude of the PSD average has no physical significance; only their relative values are of importance here. As shown in Table 1, there are three castings that showed hot tears. Two of the castings (cases 1 and 2) have the smallest arm width of 0.5″ (1.27 cm). The small arm width causes the accumulated strain to be larger than in the other cases. Ultimately, the arms with the smaller cross section will yield more easily and form a crack. The third casting that tore in the experiments was case 8 with the longest arm length (and intermediate arm width) and largest leg width. As mentioned before, the long arm length causes a large strain, while the large leg width increases the hot spot size and thus, the time over which the critical area is vulnerable to hot tearing. All of these effects appear to be captured by the present hot tear indicator.

4.2. Effect of feeding

Cases 8 and 9 illustrate the effect of feeding on the PSD predictions. In case 9, a riser is added on top of the 2.0″ wide leg of case 8 (see Fig. 2). The resulting PSD predictions are compared in Fig. 6a (case 8) and Fig. 6c (case 9). As expected,

Fig. 5. Predicted PSD distribution for a 36″ (91.44 cm) arm length and 1.0″ (2.54 cm) arm width, with 2.0″ (5.08 cm) (a) and 1.0″ (2.54 cm) (b) wide legs; the two X-ray views are cuts at the mid-plane and only show PSD percentages greater than 0.5%.

8 (Fig. 5a), a large region of PSD is predicted at the location of the hot tear in the corresponding casting experiment (Fig. 4). Fig. 5b shows that a region of PSD is also predicted for case 7, but the PSD values are much smaller than in case 8. This indicates that lower PSD values do not lead to hot tears. Note
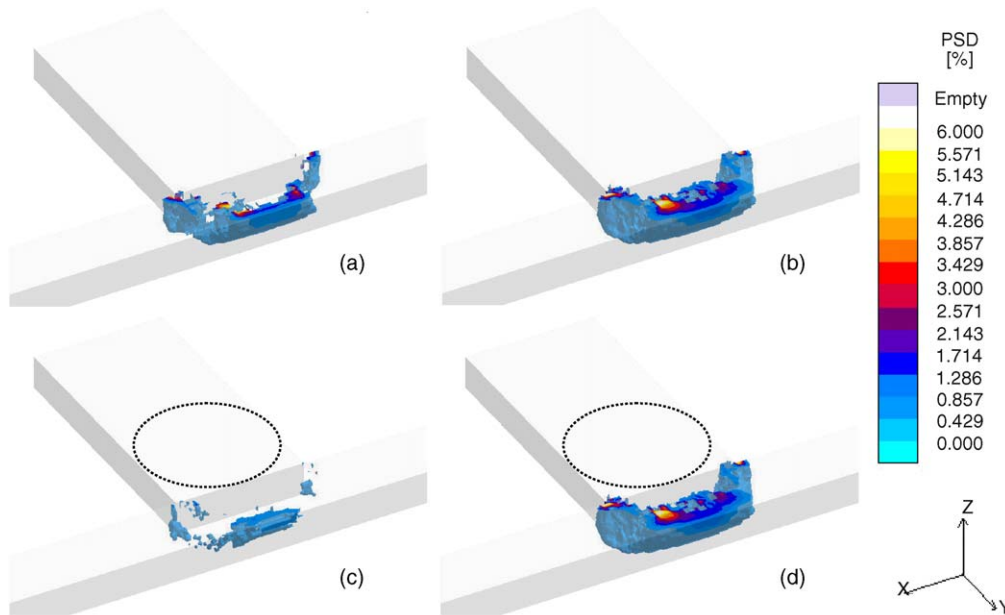

Fig. 6. Comparison of predicted PSD distributions for: (a) case 8; (b) case 8b; (c) case 9; (d) case 9b; cases 8b and 9b (right panels) use a coherency temperature integration limit that does not consider liquid feeding; cases 9 and 9b (lower panels) use a riser on top of the leg section as indicated by the circle; all four X-ray views are cuts at the mid-plane and only show PSD percentages greater than 0.5%.

the feeding of the hot spot area by the riser significantly reduces the PSD predictions relative to the case without a riser. The present hot tear indicator can predict this effect because the strain rates are only integrated, when the feeding flow is cut off (i.e., $f_p^l > 0$). Table 1 shows that the average PSD value due to the addition of the riser decreases from 1.53 to 0.78%.

To further demonstrate the importance of including the feeding effect in the present hot tear prediction, another two simulations (cases 8b and 9b) were performed, where the lower integration limit in Eq. (7) (i.e., $f_p^l > 0$) was replaced by a limit that is based on a critical mush coherency temperature. The new lower integration limit is the time at which the local temperature reaches the coherency temperature, i.e., $T < T_{\mathrm{coherent}}$, regardless of the availability of liquid feeding. The coherency temperature is defined here as the temperature where the solid fraction is equal to 0.82; it can be expected that approximately at this solid fraction the dendritic network begins to transmit stresses [3]. By changing the integration limit as described above, the strain rate may be integrated when feeding is still available and the hot tear may be healed; furthermore, integration will not start until the coherency temperature is reached even if feeding is already cut off. Fig. 6 shows that the change in the lower integration limit has little effect on the PSD predictions in the absence of the riser (compare Fig. 6a and b). This simply indicates that in the absence of the riser the time at which the coherency temperature is reached is approximately the same as the time when porosity starts to form. On the other hand, in the presence of the riser (case 9), the change in the lower integration limit has a large effect on the PSD predictions (compare Fig. 6c and d). When using the lower integration limit based on the coherency temperature, the PSD predictions are relatively unchanged by the addition of the riser (compare Fig. 6b and d). The average PSD values in Table 1 further support the above observations. The average PSD for cases 8b and 9b with the coherency temperature integration limit are of the same magnitude, indicating that the presence of feeding is not taken into account when using this integration limit. Thus, incorporating liquid metal feeding into the hot tear indicator, through the use of the $f_p^l > 0$ integration limit, is of great importance. Certainly, a more detailed consideration of the mechanical behavior of the mush and the mush coherency is nonetheless warranted for future studies.

5. Conclusions

A new hot tear indicator, PSD, based on a continuity approach is introduced. The PSD indicator is the integration of the vol-

umetric mechanical strain rate after liquid metal feeding is cut off. The PSD indications are initiation sites for hot tears. PSD is demonstrated to be sensitive to some known factors affecting hot tearing. The indications increase for increasing strain and unfed hot spots.

This indicator can be used in defect analysis for simulated casting geometries and careful attention should be paid to regions containing significant PSD. This porosity due to solid deformation is a physically sensible explanation for hot tears and may lead to a development of a reasonable prediction of hot tearing of steel castings.

References

[1] C.W. Briggs, Hot Tears in Steel Castings, Steel Founders' Society of America, Crystal Lake, IL, USA, 1968.
[2] A. Chojecki, I. Telejko, T. Bogacz, Theor. Appl. Fract. Mech. 27 (1997) 99–105.
[3] M. Rappaz, J.-M. Drezet, M. Gremaud, Metall. Mater. Trans. A 30A (1999) 449–455.
[4] C.L. Martin, M. Braccini, M. Suery, Mater. Sci. Eng. A325 (2002) 292–301.
[5] C.W. Briggs, Steel Founders' Society of America Research Report, No. 38, Technical Research Committee, Crystal Lake, IL, USA, February 1957.
[6] H. Hiebler, C. Bernhard, Steel Res. 70 (1999) 349–355.
[7] K. Nakayama, M. Kinefuchi, K. Tsutsumi, in: B.G. Thomas, C. Beckermann (Eds.), Modeling of Casting, Welding and Advanced Solidification Processes, vol. VIII, Warrendale, PA, 1998.
[8] A. Mo, M. M'Hamdi, H.G. Fjaer, in: D.M. Stefanescu, J.A. Warren, M.R. Jolly, M.J.M. Krane (Eds.), Modeling of Casting, Welding and Advanced Solidification Processes, vol. X, Warrendale, PA, 2003, pp. 199–206.
[9] MAGMAsoft, MAGMA GmbH, Kackerstrasse 11, 52072 Aachen, Germany.
[10] K. Carlson, Z. Lin, R. Hardin, C. Beckermann, G. Mazurkevich, M. Schneider, in: D.M. Stefanescu, J.A. Warren, M.R. Jolly, M.J.M. Krane (Eds.), Modeling of Casting, Welding and Advanced Solidification Processes, vol. X, Warrendale, PA, 2003, pp. 295–302.